A NOVEL METHOD FOR CALCULATING NUMBER BUILDUP FACTOR IN GAMMA-RAY TRANSMISSION MEASUREMENTS USING NARROW BEAM GEOMETRY

by

Huynh Dinh CHUONG [1,2,3*], ***Le Thi Ngoc TRANG*** [1,2,3], ***Nguyen Thi Truc LINH*** [1,2,3], ***Vo Hoang NGUYEN*** [2,3], ***and Tran Thien THANH*** [2,3]

[1] Nuclear Technique Laboratory, University of Science, Ho Chi Minh City, Vietnam
[2] Faculty of Physics and Engineering Physics, University of Science, Ho Chi Minh City, Vietnam
[3] Vietnam National University, Ho Chi Minh City, Vietnam

Scientific paper
https://doi.org/10.2298/NTRP2403185C

In this article, we present a novel method to calculate the number buildup factor for arbitrary materials in gamma-ray transmission measurements using a narrow beam geometry. The MCNP6 code was used to simulate photon transport within a collimated transmission configuration, which included a NaI(Tl) scintillation detector paired with a ^{137}Cs or ^{60}Co radioactive source. From these simulations, the number buildup factor values were computed for various materials at gamma-ray energies of 661.7 keV, 1173.2 keV, and 1332.5 keV, with sample thicknesses ranging from 0.1-7.0 cm. At each specific gamma-ray energy and material, the number buildup factor values exhibited a strong linear relationship with the sample thickness. Furthermore, the slope of these linear relationships can be expressed as a product of mass density and a cubic polynomial function of the atomic number. Based on these findings, we developed a fitting formula to calculate the number buildup factor using the input variables of sample thickness, mass density, and atomic number. The accuracy of the fitting formula was evaluated by comparing its results with number buildup factor values computed by MCNP6 code. The comparison showed relative deviations below 1 % for all the investigated cases, demonstrating the high accuracy and reliability of the fitting formula.

Key words: gamma-ray transmission, Monte Carlo simulation, MCNP6, NaI(Tl) detector, narrow beam geometry, number buildup factor

INTRODUCTION

Gamma-ray transmission (GT) technique is extensively used in non-invasive and non-destructive methods to measure the properties of materials. The significance of this technique has been well acknowledged across various applications, including industrial quality control, agriculture, and radiation protection. In industrial quality control, the GT technique is crucial for accurately determining the thickness [1-4], density [5-8], and porosity [9, 10] of samples. This helps to enhance production efficiency and ensures that industrial products consistently meet stringent quality standards. In agriculture, the GT technique is an efficient tool for analysing soil parameters [11-13]. It provides valuable insights into soil characteristics, aiding in the optimization of agricultural practices. Radiation protection has become a crucial topic in recent years, focusing on ensuring safe environments and minimizing radiation exposure risks for those working with nuclear reactors, radiotherapy facilities, and nuclear waste management. Consequently, researchers are actively developing different materials to improve shielding against gamma rays [14-21]. In these studies, the GT measurements were used to determine the mass attenuation coefficient (MAC) at gamma-ray energies of 661.7 keV, 1173.2 keV, and 1332.5 keV. The MAC is a fundamental parameter for evaluating the gamma-ray shielding properties, helping researchers to identify materials with superior shielding capabilities.

In the GT measurements, gamma rays with an energy E_0 are typically collimated into a narrow beam as they traverse through the absorbing medium. A portion of these gamma rays will undergo interactions such as photoelectric absorption, Compton scattering, Rayleigh scattering, and pair production within the medium, while the remainder, known as transmitted gamma rays, pass through without any interaction. Secondary photons, including annihilation gamma

* Corresponding author, e-mail: hdchuong@hcmus.edu.vn

rays, fluorescence X-rays, and scattered gamma rays, may reach the detector. In particular, Compton or Rayleigh scattered gamma rays with small angles have energies close to E_0, making them indistinguishable from the transmitted gamma rays due to energy resolution limits of detector. Previous studies [22, 23] have found that the influence of scattered gamma rays cannot be ignored in GT measurements, even with narrow beam geometries, for gamma-ray energies in the ranges of 8-60 keV and 661.7-1332.5 keV. Additionally, these studies concluded that discrepancies between measured and computed values of the MAC are due to the intermixing of scattered gamma rays with transmitted gamma rays reaching the detector. Therefore, carefully considering the contribution of scattered gamma rays is essential to ensure the precision of measured results in applications utilizing the GT technique.

The concept of the buildup factor was first introduced by White [24]. Depending on the physical quantity of interest, buildup factor can be classified into four categories: number buildup factor (NBF), exposure buildup factor (EBF), energy absorption buildup factor (EABF), and dose buildup factor [25]. From the perspective of applying the GT technique to non-destructive testing, the (NBF) is used to account for the contribution of scattered gamma rays to the total intensity of gamma rays with energies approximately E_0 reaching the detector. It is defined as the ratio of the total intensity of gamma rays (transmitted plus scattered gamma rays) to the intensity that would be calculated if only the transmitted gamma rays were present. In applications requiring high precision, the NBF is added as a correction factor to the Lambert-Beer law, enabling accurate descriptions of the relationship between peak areas in measured spectra and the properties of the samples under examination. Therefore, developing a convenient and effective method to calculate the NBF for GT measurements with narrow beam geometry is essential.

Monte Carlo simulation is one of the most reliable methods for calculating the NBF. The MCNP code, which is developed based on the Monte Carlo simulation method, has been widely utilized to compute buildup factors for various geometrical configurations, material types, and gamma-ray energies [26-28]. Over the years, Los Alamos National Laboratory has continuously upgraded the MCNP code, releasing new versions that incorporate additional features, provide more detailed descriptions of physical interactions, and update the databases [29]. Therefore, the MCNP code, particularly the latest versions, is an excellent choice for computing the NBF using Monte Carlo simulation method. However, Monte Carlo simulations require long computation times. For example, completing the simulation for one of our MCNP input files using a computer with an Intel® Core™ i9 Processor takes approximately five days. Such long computation times make the Monte Carlo simulation method unsuitable for calculating NBF across arbitrary cases with variations in material type, absorption thickness, and gamma-ray energy. Instead, this method should be reserved for specific cases, which can then be used to create a reference database for broader applications.

One solution to the above problem is to develop fitting formulas based on existing data, enabling the convenient and rapid calculation of NBF for various scenarios. In the past, researchers have proposed several fitting formulas, such as the Taylor form [30], Berger form [31], and Geometric Progression form [32], to calculate buildup factors for the geometry of a point isotropic source in an infinite homogeneous medium. However, these formulas are unsuitable for GT measurements using narrow beam geometries. To the best of our knowledge, very few studies have focused on evaluating buildup factors in narrow beam geometries. This gap in research may lead to underestimating the influence of the buildup factors, which is often assumed to be equal to 1 in such geometries. It should be emphasized that this assumption is unrealistic because most practical geometries cannot eliminate the contribution of scattered gamma rays, as demonstrated in studies [21, 22]. Furthermore, we were unable to find any fitting formulas for the buildup factors in narrow beam geometries in the existing literature.

In the present study, we introduce a novel method that combines Monte Carlo simulation with fitting formula to calculate the NBF for arbitrary materials in GT measurements using narrow beam geometry. Initially, the MCNP6 code is used to compute the NBF for various materials at gamma-ray energies of 661.7 keV, 1173.2 keV, and 1332.5 keV, with sample thicknesses ranging from 0.1-7.0 cm. The simulation results provide practical insights into NBF values across different material types, thicknesses, and gamma-ray energies. Subsequently. The NBF values for single-element materials serve as a reference database for developing a fitting formula. This formula enables the rapid calculation of the NBF based on input variables such as thickness, mass density, and effective atomic number. The accuracy of the fitting formula is evaluated by comparing its results with NBF values computed by MCNP6 code for materials not included in the database.

MATERIALS AND METHODS

Theoretical background

In this section, we present theoretical background to understand the relationship between the NBF and the properties of the sample, including thickness, mass density, and composition. For GT measurements using narrow beam geometry, the gamma rays with energies approximately E_0 reaching the detector consist of two

components: the transmitted gamma rays and the scattered gamma rays. Before reaching the detector, the scattered gamma rays may undergo either single Compton or Rayleigh scattering, or multiple Compton and Rayleigh scattering within the sample. It should be noted that the probability of gamma rays undergoing multiple scatterings while retaining energies of approximately E_0 and then reaching the detector is very low. Therefore, in the theoretical formulas, we only consider the contribution of gamma rays that have undergone single Compton or Rayleigh scattering.

The intensity of the transmitted gamma rays, denoted as I_{Tran}, can be expressed by the Lambert-Beer law.

$$I_{\text{Tran}} = I_0 \mathrm{e}^{-\mu_m(E_0)\rho d} \tag{1}$$

Figure 1 illustrates the single Compton or Rayleigh scattering at point P within the sample. Here, point P acts as a source emitting secondary gamma rays. The intensity of Compton and Rayleigh scattered gamma rays traveling from point P to the detector, denoted as dI_{Scat}, is calculated by eq. (2)

$$dI_{\text{Scat}} = I_0 \rho \frac{N_A}{A} \mathrm{e}^{-\mu_m(E_0)\rho x} \mathrm{d}x \int_{\Omega} \left[\left(\frac{\mathrm{d}\sigma_a^C}{\mathrm{d}\Omega} \right)_\theta \mathrm{e}^{-\mu_m(E_0)\rho x'} + \left(\frac{\mathrm{d}\sigma_a^R}{\mathrm{d}\Omega} \right)_\theta \mathrm{e}^{-\mu_m(E_0)\rho x'} \right] \mathrm{d}\Omega \tag{2}$$

where I_0 is the intensity of the incident gamma rays, μ_{m} – the MAC of the sample, ρ and d are the mass density and thickness of the sample, respectively, x and x' are the path lengths of incident gamma rays and scattered gamma rays within the sample, respectively, dx – the differential path length of the incident gamma rays from point P, during which scattered gamma rays are emitted, $(\mathrm{d}\sigma_a^C/\mathrm{d}\Omega)_\theta$ and $(\mathrm{d}\sigma_a^R/\mathrm{d}\Omega)_\theta$ are the differential cross sections of Compton scattering and Rayleigh scattering with a scattering angle θ, respectively, Ω – the solid angle subtended by the detector at point P, and dΩ – the differential solid angle around scattered gamma rays with a scattering angle θ, A – the atomic weight, N_{A} is Avogadro's constant, E_0 – the energy of the incident gamma rays and the Rayleigh scattered gamma rays, E – the energy of the Compton scattered gamma rays.

The intensity of Compton and Rayleigh scattered gamma rays reaching the detector, denoted as I_{Scat}, is calculated by integrating dI_{Scat} over the entire thickness of the sample

$$I_{\text{Scat}} = \int \mathrm{d}I_{\text{Scat}} = I_0 \rho \frac{N_A}{A} \int_0^d \mathrm{e}^{-\mu_m(E_0)\rho x} \mathrm{d}x \int_{\Omega} \left[\left(\frac{\mathrm{d}\sigma_a^C}{\mathrm{d}\Omega} \right)_\theta \mathrm{e}^{-\mu_m(E)\rho x'} + \left(\frac{\mathrm{d}\sigma_a^R}{\mathrm{d}\Omega} \right)_\theta \mathrm{e}^{-\mu_m(E_0)\rho x'} \right] \mathrm{d}\Omega \tag{3}$$

In eq. (3), the term Ω is a function dependent on x, the sample-to-detector distance (denoted as L), and the diameter of the detector collimator (denoted as D), which is given by eq. (4)

$$\Omega = \frac{\pi D^2}{4(d - x + L)^2} \tag{4}$$

with a given sample thickness, Ω varies over a range from $\pi D^2/[4(d+L)^2]$ sr to $\pi D^2/(4L^2)$ sr.

Besides, the terms $(\mathrm{d}\sigma_a^C/\mathrm{d}\Omega)_\theta$, $(\mathrm{d}\sigma_a^R/\mathrm{d}\Omega)_\theta$, $\mu_{\text{m}}(E)$, and x' are functions dependent on the scattering angle θ. The scattering angle θ can vary from 0 to $\theta_{\max} = arc\cos\left(L/\sqrt{L^2 + (D/2)^2}\right)$.

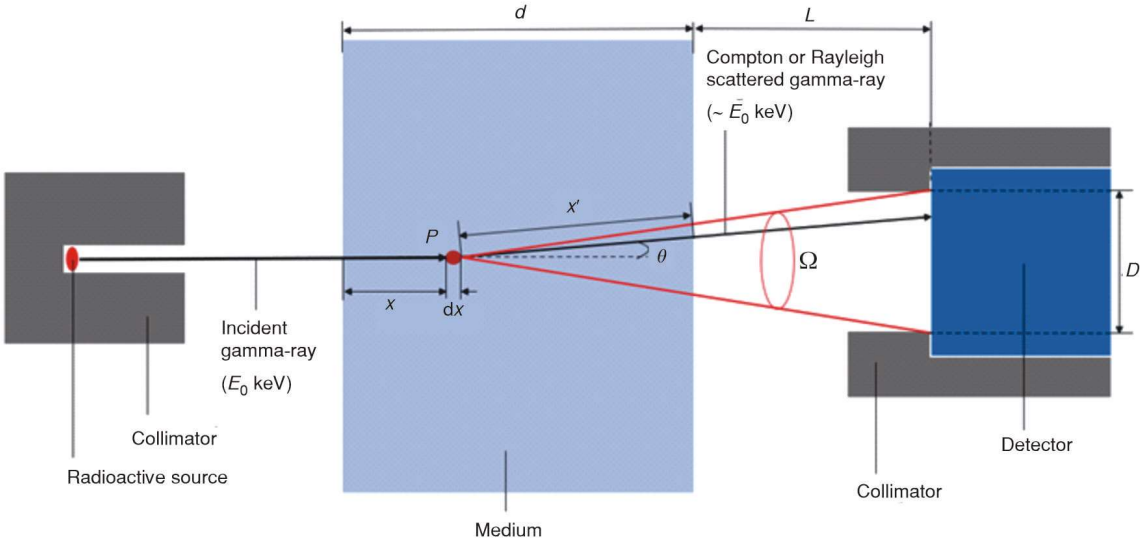

Figure 1. Illustration of a single Compton or Rayleigh scattering in GT measurements using narrow beam geometry

The presence of these variables complicates the integrals in eq. (3), making it impossible to represent them using analytical expressions. However, eq. (3) can be simplified if the measurement geometry meets the following conditions (i) $L \gg d$ and (ii) $L \gg D$. When condition (i) is satisfied, Ω can be treated as a constant with its value approximately equal to $\pi D^2/(4L^2)$. When condition (ii) is satisfied, the scattering angle $\theta_{\max}$ approaches 0. This means that only gamma rays scattered at very small angles can reach the detector. Consequently, we can use the approximate expressions (5)-(7)

$$\cos\theta \approx 1 \Rightarrow x' = \frac{d-x}{\cos\theta} \approx d - x \tag{5}$$

$$E = \frac{E_0}{1+\frac{E_0}{511}(1-\cos\theta)} \approx E_0 \Rightarrow \mu_\mu(E) \approx \mu_m(E_0) \tag{6}$$

$$\left(\frac{\mathrm{d}\sigma_a^C}{\mathrm{d}\Omega}\right)_\theta \approx \text{const} \text{ and } \left(\frac{\mathrm{d}\sigma_a^R}{\mathrm{d}\Omega}\right)_\theta \approx \text{const} \tag{7}$$

Applying the above approximations to eq. (3), we have eq. (8)

$$I_{\text{Scat}} \approx I_0 \mathrm{e}^{-\mu_m \rho d} \frac{N_A}{A}\left[\left(\frac{\mathrm{d}\sigma_a^C}{\mathrm{d}\Omega}\right)_\theta + \left(\frac{\mathrm{d}\sigma_a^R}{\mathrm{d}\Omega}\right)_\theta\right]\frac{\pi D^2}{4L^2}\rho\mathrm{d} \tag{8}$$

The total intensity of gamma rays with energies approximately E_0 reaching the detector, denoted as I, can be calculated using eq. (9)

$$I = I_{\text{Tran}} + I_{\text{Scat}} =$$
$$= I_0 \mathrm{e}^{-\mu_m \rho d}\left\{1 + \frac{N_A}{A}\left[\left(\frac{\mathrm{d}\sigma_a^C}{\mathrm{d}\Omega}\right)_\theta + \left(\frac{\mathrm{d}\sigma_a^R}{\mathrm{d}\Omega}\right)_\theta\right]\frac{\pi D^2}{4L^2}\rho\mathrm{d}\right\} \tag{9}$$

Finally, the relationship between the NBF (denoted as B) and the sample properties can be expressed as eq. (10)

$$B = \frac{I}{I_{\text{Tran}}} =$$
$$= 1 + \frac{N_A}{A}\left[\left(\frac{\mathrm{d}\sigma_a^C}{\mathrm{d}\Omega}\right)_\theta + \left(\frac{\mathrm{d}\sigma_a^R}{\mathrm{d}\Omega}\right)_\theta\right]\frac{\pi D^2}{4L^2}\rho\mathrm{d} = 1 + k\rho d \tag{10}$$

with

$$k = \frac{N_A}{A}\left[\left(\frac{\mathrm{d}\sigma_a^C}{\mathrm{d}\Omega}\right)_\theta + \left(\frac{\mathrm{d}\sigma_a^R}{\mathrm{d}\Omega}\right)_\theta\right]\frac{\pi D^2}{4L^2} \tag{11}$$

For single-element materials with atomic number Z, the Compton scattering cross section is proportional to Z, while the Rayleigh scattering cross section is proportional to Z^2 [33]. In addition, the ratio of atomic number to atomic weight (Z/A) varies with Z, as shown in fig. 2. The atomic weights of various elements with Z ranging from 2 to 100 are sourced from reference [34]. Consequently, for a fixed GT geometry, the term k can be considered a function of Z.

For multi-element materials such as alloys, mixtures, and compounds, the atomic number is replaced by a parameter known as the effective atomic number, denoted as Z_{eff}. This parameter is typically calculated by taking into account the proportion of each element in a material and their respective atomic numbers, resulting in a single representative value. In radiation physics, Z_{eff} is crucial for reflecting the overall behaviour of a multi-element material in terms of interaction with radiation. Numerous theoretical expressions for calculating the Z_{eff} are available in the literature [35-38]. In this study, we apply eq. (12) to determine Z_{eff} and evaluate its applicability in calculating the NBF.

$$Z_{\text{eff}} = \sum_{i=1}^{n}\left[\frac{\left(\frac{w_i}{A_i}Z_i\right)}{\sum_{i=1}^{n}\left(\frac{w_i}{A_i}Z_i\right)}Z_i^{3.4}\right]^{1/3.4} \tag{12}$$

where w_i, Z_i, and A_i are the weight fraction, atomic number, and atomic weight of the i-th element, respectively, n – the number of elements present in the material.

Monte Carlo simulations

We used the MCNP6 code to simulate photon transport within a GT configuration, as described in fig. 3. This simulation configuration was designed to replicate our actual GT system, with detailed information provided in a previous study [4]. In the simulations, the source is set to emit photons at an energy of 661.7 keV

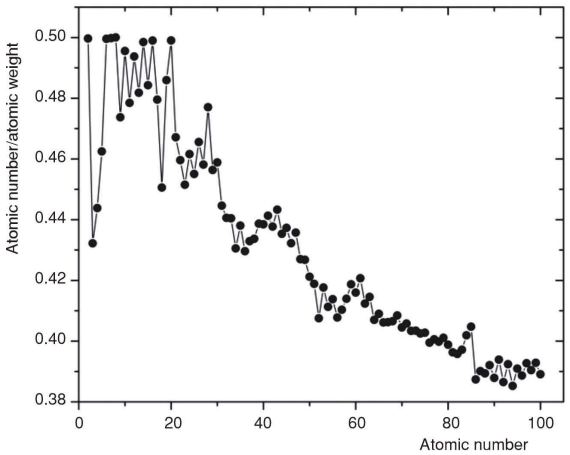

Figure 2. The variation of the ratio of atomic number to atomic weight with respect to atomic number [34]

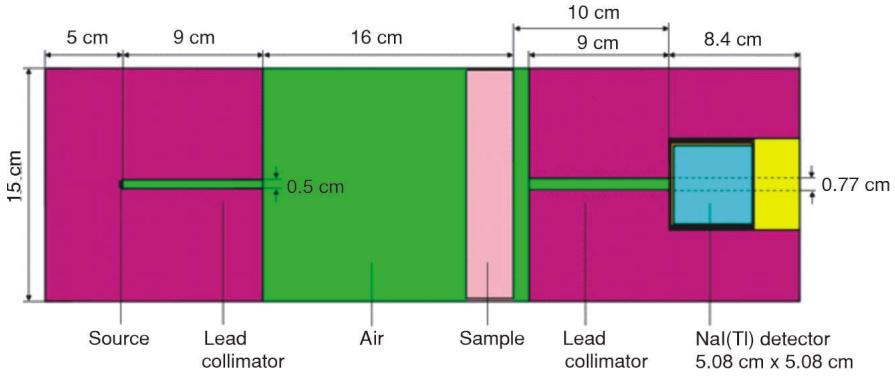

Figure 3. Simulation configuration of the GT system in this study

for ^{137}Cs, or at both 1173.2 keV and 1332.5 keV for ^{60}Co. A model of the NaI(Tl) scintillation detector was established based on the optimized parameters from our previous study [39]. Detailed physics of the photon interactions, encompassing photoelectric effect, incoherent scattering, coherent scattering, pair production, bremsstrahlung photon and fluorescence emission following photoelectric absorption, were included in the simulations. The databases for photon interactions and atomic relaxation are sourced from ENDF/B-VI.8. The cut-off energy for photon transport was set at 1 keV. To achieve good statistical accuracy with uncertainties below 0.5 % for the data of interest, each simulation emitted 10 billion photons from the source.

The F8 tally, available in the MCNP6 code, was employed to obtain the pulse height distribution spectra for the NaI(Tl) detector in the simulation configuration. Additionally, the simulations integrated crucial characteristics of experimental spectra obtained from an actual NaI(Tl) scintillation detector, including the position and width of the peaks. It should be emphasized that the previous study [4] confirmed an excellent agreement between the experimental spectra and the simulated spectra. This indicates that the results obtained from this simulation configuration are fully applicable to the real GT system.

To obtain diverse data for evaluating the NBF, we conducted simulations on 32 different sample material types. This included 24 single-element materials with atomic numbers ranging from 3 to 83 and 8 multi-element materials with effective atomic numbers ranging from 12.70 to 74.27. The atomic number and mass density of the single-element materials are given in tab. 1. The composition, elemental weight fraction, effective atomic number, calculated by eq. (12), and mass density of the multi-element materials are presented in tab. 2. For each material type, the samples have dimensions of 10 cm × 15 cm, with thicknesses of 0.1 cm, 0.5 cm, 1.0 cm, 1.5 cm, 2.0 cm, 2.5 cm, 3.0 cm, 3.5 cm, 4.0 cm, 4.5 cm, 5.0 cm, 5.5 cm, 6.0 cm, 6.5 cm, and 7.0 cm. The sample was positioned perpendicular to the gamma-ray beam, with a sample-to-detector distance of 10 cm. Additionally, simulations were also performed without a sample present between the source and the detector.

Calculation of the number buildup factor using simulation data

To calculate the NBF, it is essential to know both the total intensity of gamma rays (including transmitted and scattered gamma rays) and the intensity of the transmitted gamma rays. The total intensity of gamma rays reaching the detector can be determined by analysing the areas under the relevant peaks in the simulated spectra and applying the full-energy peak efficiencies of the detector. However, from the simulated spectra, we cannot separately estimate the intensities of only transmitted gamma rays or only scattered gamma rays.

Table 1. Atomic number and mass density of single-element materials used in the Monte Carlo simulations

Material	Atomic number	Mass density [gcm^{-3}]	Material	Atomic number	Mass density [gcm^{-3}]
Lithium	3	0.534	Nickel	28	8.902
Beryllium	4	1.848	Copper	29	8.96
Carbon	6	2.0	Zinc	30	7.14
Sodium	11	0.971	Germanium	32	5.323
Magnesium	12	1.74	Zirconium	40	6.506
Aluminum	13	2.699	Tin	50	7.31
Silicon	14	2.33	Terbium	65	8.229
Scandium	21	2.989	Thulium	69	9.321
Titanium	22	4.54	Lutetium	71	9.84
Manganese	25	7.44	Hafnium	72	13.31
Iron	26	7.874	Lead	82	11.35
Cobalt	27	8.9	Bismuth	83	9.747

Table 2. Composition, effective atomic number, and mass density of multi-element materials used in the Monte Carlo simulations

Material	Composition (Z_i – w_i)	Effective atomic number	Mass density [gcm^{-3}]
Silicon carbide	6-0.299547, 14-0.700453	12.70	3.21
7075-T6 aluminum alloy	12-0.025, 13-0.8925, 14-0.00234, 22-0.00117, 24-0.0023, 25-0.00176, 26-0.00293, 29-0.016, 30-0.056	16.27	2.81
Titanium carbide	6-0.200548, 22-0.799452	20.51	4.94
321 stainless steel	6-0.0008, 14-0.01, 15-0.00045, 16-0.0003, 22-0.0015, 24-0.18, 25-0.02, 26-0.67695, 28-0.11	25.81	8.0
NRX 600 (Ni-Cr-Fe alloy)	24-0.15, 26-0.08, 28-0.77	27.34	8.55
C27000 copper alloy	26-0.0007, 29-0.6575, 30-0.3408, 82-0.001	29.59	8.47
Bismuth germanate	8-0.154126, 32-0.17482, 83-0.671054	72.89	7.13
Lead tungstate	8-0.140642, 74-0.404011, 82-0.455347	74.27	8.24

To address this issue, we assume that high-energy gamma rays are not significantly attenuated when traveling through dry air. Indeed, the linear attenuation coefficients of gamma rays with energies of 661.7 keV, 1173.2 keV, and 1332.5 keV in dry air are 0.000093 cm^{-1}, 0.000071 cm^{-1}, and 0.000066 cm^{-1}, respectively. These very low values indicate that the intensity of the gamma rays will not change significantly after traveling 35 cm from the source to the detector through dry air. Therefore, the intensity of the gamma rays reaching the detector in the absence of a sample can be considered equal to the intensity of the incident gamma rays (I0). Under this assumption, eq. (9) can be rewritten to yield eq. (13)

$$N = I\varepsilon t = I_0\varepsilon t(\mathrm{e}^{-\mu_m\rho d})B = N_0(\mathrm{e}^{-\mu_m\rho d})B \quad (13)$$

where N and N_0 are the areas under the relevant peaks in the simulated spectra obtained with and without a sample, respectively, ε – the full-energy peak efficiency of the detector, t – the spectrum acquisition time.

Consequently, the NBF can be calculated by

$$B = \frac{N}{N_0\mathrm{e}^{-\mu_m\rho d}} \quad (14)$$

The uncertainty of the NBF, denoted as σ_B, is determined according to the law of uncertainty propagation

$$\sigma_B = \sqrt{\frac{1}{N_0^2(\mathrm{e}^{-\mu_m\rho d})^2}\sigma_N^2 + \frac{N^2}{N_0^4(\mathrm{e}^{-\mu_m\rho d})^2}\sigma_{N_0}^2} \quad (15)$$

where σ_N and σ_{N_2} are the uncertainties of N and N_0, respectively. Here, $\sigma_N = 3.89\sqrt{N}$ and $\sigma_{N_0} = 3.89\sqrt{N_0}$. It should be noted that the values of μ_m, ρ and d have no uncertainties. Consequently, in eq. (15), we only consider the uncertainties of N and N_0.

To calculate the NBF and its uncertainty using eqs. (14) and (15), it is necessary to know the MAC values of the materials under examination. In this study, we used the XCOM web program, developed by NIST [40], to calculate the MAC at gamma-ray energies of 661.7 keV, 1173.2 keV, and 1332.5 keV.

Besides, we analysed the simulated spectra to determine the areas under the relevant peaks. For the 661.7 keV peak of the ^{137}Cs source, we selected a region of interest (ROI) spanning from the channel 823 to the channel 974 in each spectrum, as illustrated in fig. 4(a). In the cases of the ^{60}Co source, the ROI spanned from the channel 1465 to channel 1664 for the 1173.2 keV peak and from the channel 1666 to the channel 1879 for the 1332.5 keV peak, as illustrated in fig. 4(b). The areas under the relevant peaks were then determined by summing the counts within each ROI.

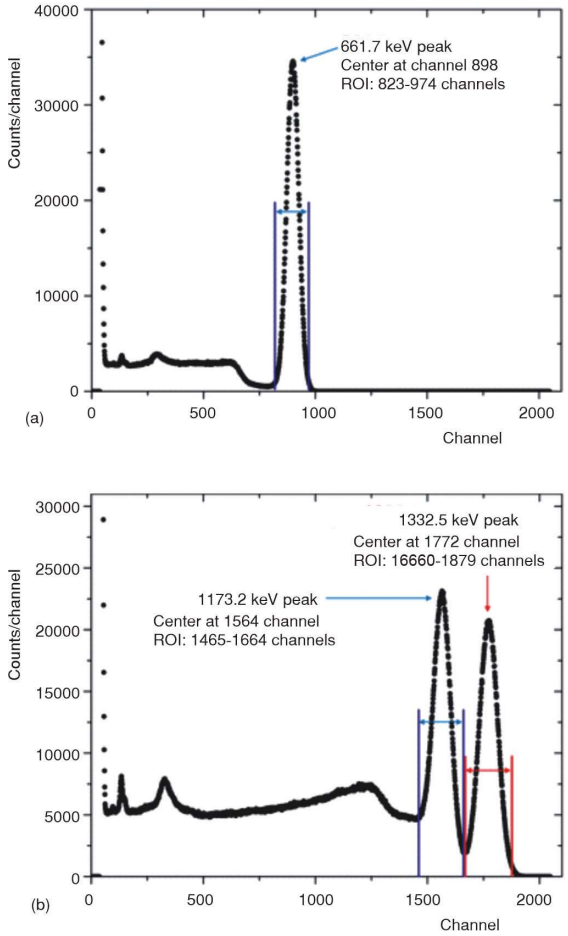

Figure 4. The regions of interest in the simulated spectra for: (a) ^{137}Cs source and (b) ^{60}Co source

RESULTS AND DISCUSSIONS

Development of a fitting formula for calculating the number buildup factor

Using data obtained from the Monte Carlo simulations, we calculated the NBF and its uncertainty for various material types, sample thicknesses, and gamma-ray energies. Subsequently, for a given gamma-ray energy, we analysed the variation trends of the NBF with respect to sample thickness, mass density, and atomic number of the material. Based on these trends, we proposed a fitting formula to calculate the NBF.

Figure 5 shows the values of the NBF for single-element materials at an energy of 1173.2 keV, across the sample thicknesses ranging from 0.1 cm to 7.0 cm. Similar results are also observed at the energies of 661.7 keV and 1332.5 keV. The NBF values start at approximately 1 for small sample thicknesses and increase linearly as the sample thickness increases. This trend is consistent for all material types and gamma-ray energies examined. Notably, this finding agrees with the theoretical background outlined in eq. (10), which shows a linear relationship between the NBF and the sample thickness.

Based on the previous analysis, we employed the least-squares method to fit the NBF values against sample thickness for single-element materials using the linear function

$$B_{\text{Fiting}} = 1 + Sd \tag{16}$$

Here, the symbol B_{Fitting} is used to distinguish it from the symbol B in eq. (14); and S is a fitting parameter that represents the slope of the linear relationships. Values of the parameter S and its uncertainty are determined by the least-squares method.

The results show a good agreement between the data points and the linear fitting lines, with R^2 approximately 1.0 for all the investigated cases. In addition, the average relative deviations (RD) between the NBF values and the fitting values are 0.11 %, 0.05 %, and 0.04 % for gamma-ray energies of 661.7 keV, 1173.2 keV, and 1332.5 keV, respectively.

Besides, tab. 3 presents values of the parameter S and its uncertainties for the single-element materials at gamma-ray energies of 661.7 keV, 1173.2 keV, and 1332.5 keV. We observe a following trend: as the mass density and atomic number of the materials increase, value of the parameter S also increases. This trend is

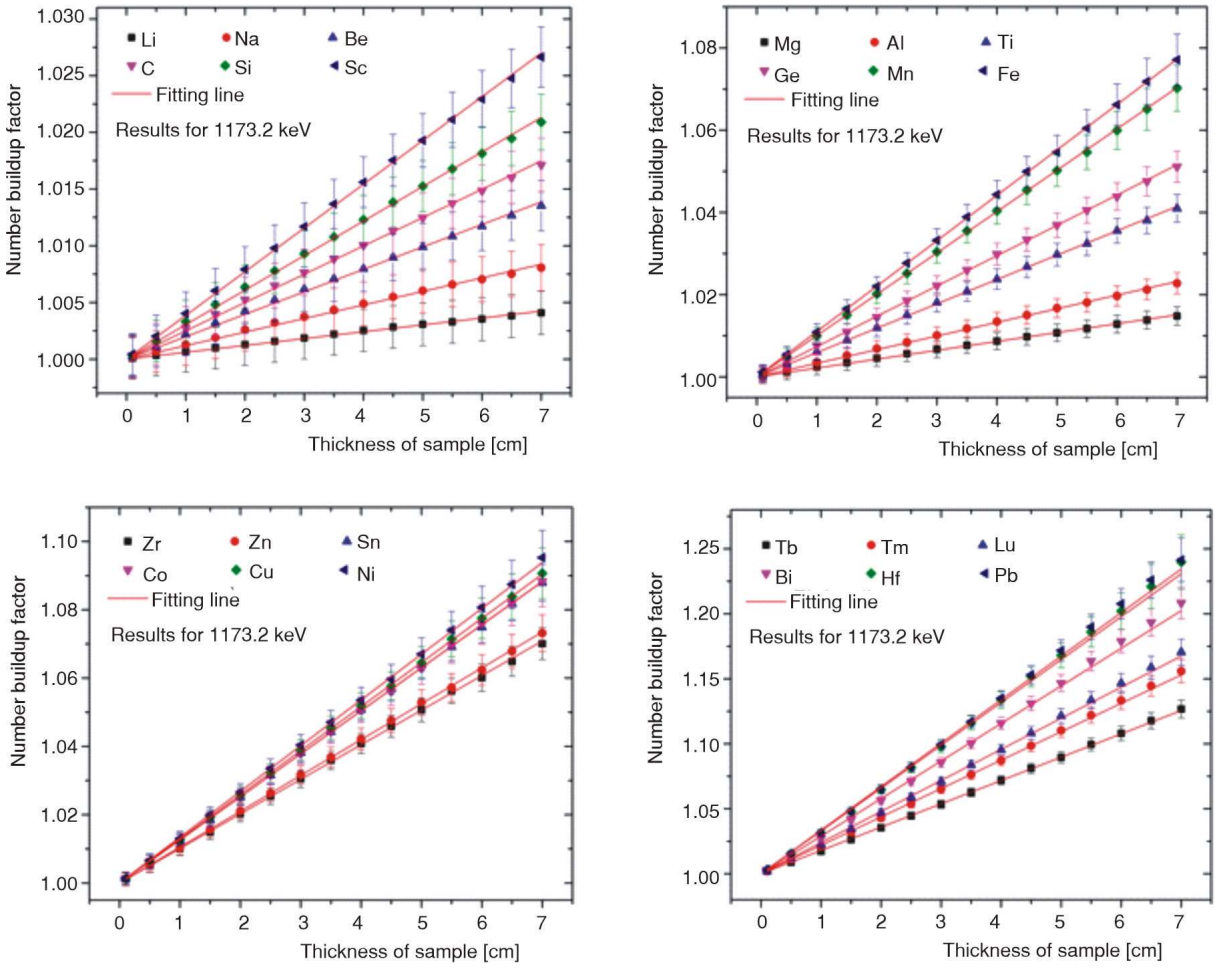

Figure 5. Dependence of the NBF on the sample thickness for single-element materials at an energy of 1173.2 keV

Table 3. Values of the parameter *S* and its uncertainty for the single-element materials at gamma-ray energies of 661.7 keV, 1173.2 keV, and 1332.5 keV

Material	Values of S [cm^{-1}] at 661.7 keV	Values of S [cm^{-1}] at 1173.2 keV	Values of S [cm^{-1}] at 1332.5 keV
Lithium	0.000304 (2)	0.000604 (6)	0.000364 (4)
Beryllium	0.000886 (5)	0.00198 (1)	0.00114 (1)
Carbon	0.001180 (4)	0.00250 (1)	0.00139 (1)
Sodium	0.000697 (2)	0.00119 (1)	0.000714 (8)
Magnesium	0.001250 (5)	0.00216 (1)	0.00125 (1)
Aluminum	0.001910 (7)	0.00331 (1)	0.00191 (1)
Silicon	0.001810 (5)	0.00304 (1)	0.00177 (1)
Scandium	0.00270 (1)	0.00386 (1)	0.00230 (2)
Titanium	0.00411 (2)	0.00592 (1)	0.00349 (3)
Manganese	0.00730 (3)	0.01005 (2)	0.00574 (5)
Iron	0.00819 (3)	0.01104 (2)	0.00640 (5)
Cobalt	0.00942 (3)	0.01260 (2)	0.00724 (5)
Nickel	0.01026 (3)	0.01340 (3)	0.00782 (5)
Copper	0.01015 (3)	0.01291 (2)	0.00755 (5)
Zinc	0.00865 (3)	0.01049 (2)	0.00624 (6)
Germanium	0.00637 (3)	0.00737 (2)	0.00437 (3)
Zirconium	0.01018 (2)	0.01012 (3)	0.00609 (4)
Tin	0.01431 (2)	0.01261 (3)	0.00772 (5)
Terbium	0.02278 (9)	0.01793 (5)	0.01079 (6)
Thulium	0.02854 (14)	0.02185 (9)	0.01309 (5)
Lutetium	0.03152 (19)	0.02392 (11)	0.01410 (5)
Hafnium	0.04354 (38)	0.03296 (21)	0.01980 (5)
Lead	0.04549 (42)	0.03348 (23)	0.01952 (4)
Bismuth	0.04023 (35)	0.02891 (18)	0.01686 (4)

Note that 0.000304 (2) means 0.000304 ± 0.000002

entirely consistent with the theoretical background. Indeed, by comparing eq. (10) and eq. (16), we can derive eq. (17)

$$S = k\rho = f(Z)\rho \tag{17}$$

It is known that the term k is a function of the atomic number Z, denoted as $f(Z)$. Therefore, the parameter S is proportional to both the mass density ρ and the function $f(Z)$. This relationship explains the observed trend. To determine the form of the function $f(Z)$, we examined the variation of the S/ρ ratio with Z for gamma-ray energies of 661.7 keV, 1173.2 keV, and 1332.5 keV, as shown in fig. 6. Subsequently, we identified the cubic polynomial function as the most suitable choice for fitting these data

$$S/\rho = A_0 + A_1 Z + A_2 Z^2 + A_3 Z^3 \tag{18}$$

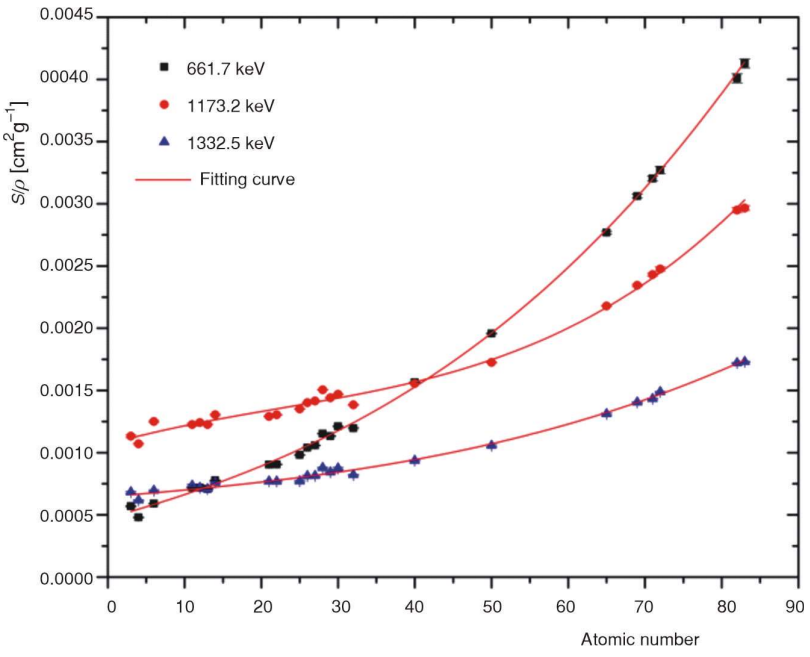

Figure 6. Dependence of the S/ρ ratio on the atomic number for single-element materials at gamma-ray energies of 661.7 keV, 1173.2 keV, and 1332.5 keV

Table 4. Values of the parameters A_0, A_1, A_2, A_3 and their uncertainties at gamma-ray energies of 661.7 keV, 1173.2 keV, and 1332.5 keV

Parameters	Values for 661.7 keV	Values for 1173.2 keV	Values for 1332.5 keV
A_0	0.00047 (3)	0.00106 (6)	0.00064 (2)
A_1	0.000017 (4)	0.000018 (6)	0.000005 (2)
A_2	0.00000013 (13)	–0.0000003 (2)	0.000000022 (56)
$A3$	0.0000000023 (14)	0.0000000047 (16)	0.0000000009 (4)

where A_0, A_1, A_2, and A_3 are fitting parameters. The values of these parameters and their uncertainties at gamma-ray energies of 661.7 keV, 1173.2 keV, and 1332.5 keV are determined using the least-squares method and are presented in tab. 4. It is evident that the value of the parameter A_i ($i = 0, 1, 2, 3$) varies with the gamma-ray energy. However, the current results are insufficient to establish a definitive relationship between these quantities.

By combining eqs. (16)-(18), we derive a fitting formula to determine the NBF

$$B_{\text{Fitting}} = 1 + (A_0 + A_1 Z + A_2 Z^2 + A_3 Z^3)\rho d \quad (19)$$

The uncertainty of B_{Fitting}, denoted as σ_{Fitting}, is determined according to the law of uncertainty propagation

$$\sigma_{\text{Fitting}} = \sqrt{(\sigma_{A_0}^2 + Z^2\sigma_{A_1}^2 + Z^4\sigma_{A_2}^2 + Z^6\sigma_{A_3}^2)\rho^2 d^2} \quad (20)$$

where σ_{A_0}, σ_{A_1}, σ_{A_2}, and σ_{A_3} are the uncertainties of A_0, A_1, A_2, and A_3, respectively.

The fitting formula, eq. (19), can be used to determine the NBF of a given sample if the sample thickness, mass density, and atomic number of the material are known. For samples composed of multi-element materials, the effective atomic number (Z_{eff}) should be used instead of the atomic number (Z) in eq. (19). Note that the fitting formula is valid for sample thicknesses ranging from 0.1 cm to 7.0 cm and for materials with atomic numbers or effective atomic numbers between 3 and 83.

Validation of the fitting formula

The fitting formula is validated by comparing its results with NBF values computed using the MCNP6 code for various multi-element materials, including silicon carbide, 7075-T6 aluminum alloy, titanium carbide, 321 stainless steel, NRX 600, C27000 copper alloy, bismuth germanate, and lead tungstate. These materials were not used in the development of the fitting formula, thereby ensuring objectivity in validation. Furthermore, their effective atomic numbers range from 12.7 to 74.27 (see tab. 2), thus providing a diverse dataset for validation.

Tables 5-12 present the NBF values calculated using both the fitting formula and the MCNP6 code, along with the (RD) between them, for the multi-element materials at gamma-ray energies of 661.7 keV, 1173.2 keV, and 1332.5 keV. The results clearly show that the fitting formula values are in excellent agreement with the MCNP6 values. The RD are less than 0.5 % for materials with effective atomic numbers below 30. For bismuth germanate ($Z_{\text{eff}} = 72.89$) and lead tungstate ($Z_{\text{eff}} = 74.27$). The RD increase slightly but remain below 1 %. These results confirm the high accuracy of the proposed fitting formula in calculating the NBF.

Table 5. Comparison of NBF values calculated using the fitting formula and MCNP6 code for silicon carbide at gamma-ray energies of 661.7 keV, 1173.2 keV, and 1332.5 keV

Thickness [cm]	Results for 661.7 keV			Results for 1173.2 keV			Results for 1332.5 keV		
	Fitting formula	MCNP6	RD [%]	Fitting formula	MCNP6	RD [%]	Fitting formula	MCNP6	RD [%]
0.1	1.0002	1.0002	0.01	1.0004	1.0005	0.01	1.0002	1.0003	0.00
0.5	1.0012	1.0011	0.01	1.0020	1.0022	0.02	1.0011	1.0013	0.01
1.0	1.0023	1.0022	0.01	1.0040	1.0044	0.04	1.0023	1.0026	0.03
1.5	1.0035	1.0034	0.00	1.0060	1.0065	0.05	1.0034	1.0039	0.04
2.0	1.0046	1.0047	0.00	1.0080	1.0085	0.05	1.0046	1.0050	0.04
2.5	1.0058	1.0058	0.00	1.0100	1.0106	0.06	1.0057	1.0062	0.05
3.0	1.0069	1.0069	0.00	1.0120	1.0127	0.07	1.0069	1.0075	0.06
3.5	1.0081	1.0081	0.00	1.0140	1.0148	0.08	1.0080	1.0085	0.05
4.0	1.0092	1.0095	0.02	1.0160	1.0169	0.09	1.0092	1.0097	0.06
4.5	1.0104	1.0105	0.01	1.0180	1.0188	0.09	1.0103	1.0109	0.06
5.0	1.0116	1.0117	0.01	1.0200	1.0210	0.10	1.0115	1.0119	0.05
5.5	1.0127	1.0125	0.02	1.0220	1.0229	0.09	1.0126	1.0129	0.03
6.0	1.0139	1.0136	0.03	1.0240	1.0249	0.09	1.0138	1.0139	0.02
6.5	1.0150	1.0146	0.04	1.0260	1.0269	0.09	1.0149	1.0149	0.01
7.0	1.0162	1.0158	0.04	1.0280	1.0288	0.08	1.0161	1.0162	0.01

Table 6. Comparison of NBF values calculated using the fitting formula and MCNP6 code for 7075-T6 aluminum alloy at gamma-ray energies of 661.7 keV, 1173.2 keV, and 1332.5 keV

Thickness [cm]	Results for 661.7 keV			Results for 1173.2 keV			Results for 1332.5 keV		
	Fitting formula	MCNP6	RD [%]	Fitting formula	MCNP6	RD [%]	Fitting formula	MCNP6	RD [%]
0.1	1.0002	1.0002	0.01	1.0004	1.0004	0.00	1.0002	1.0002	0.00
0.5	1.0011	1.0010	0.01	1.0018	1.0018	0.00	1.0010	1.0011	0.01
1.0	1.0023	1.0020	0.02	1.0036	1.0037	0.01	1.0021	1.0022	0.01
1.5	1.0034	1.0030	0.03	1.0054	1.0055	0.01	1.0031	1.0032	0.01
2.0	1.0045	1.0043	0.02	1.0072	1.0072	0.00	1.0041	1.0042	0.01
2.5	1.0056	1.0053	0.03	1.0090	1.0089	0.01	1.0052	1.0053	0.01
3.0	1.0068	1.0064	0.03	1.0108	1.0107	0.02	1.0062	1.0063	0.01
3.5	1.0079	1.0074	0.05	1.0126	1.0123	0.03	1.0073	1.0073	0.01
4.0	1.0090	1.0085	0.05	1.0144	1.0142	0.03	1.0083	1.0082	0.01
4.5	1.0101	1.0097	0.04	1.0163	1.0159	0.04	1.0093	1.0091	0.02
5.0	1.0113	1.0107	0.06	1.0181	1.0176	0.05	1.0104	1.0101	0.02
5.5	1.0124	1.0116	0.08	1.0199	1.0191	0.07	1.0114	1.0110	0.04
6.0	1.0135	1.0126	0.09	1.0217	1.0209	0.07	1.0124	1.0118	0.06
6.5	1.0146	1.0134	0.12	1.0235	1.0224	0.11	1.0135	1.0125	0.09
7.0	1.0158	1.0144	0.13	1.0253	1.0240	0.12	1.0145	1.0134	0.11

Table 7. Comparison of NBF values calculated using the fitting formula and MCNP6 code for titanium carbide at gamma-ray energies of 661.7 keV, 1173.2 keV, and 1332.5 keV

Thickness [cm]	Results for 661.7 keV			Results for 1173.2 keV			Results for 1332.5 keV		
	Fitting formula	MCNP6	RD [%]	Fitting formula	MCNP6	RD [%]	Fitting formula	MCNP6	RD [%]
0.1	1.0004	1.0003	0.01	1.0007	1.0007	0.01	1.0004	1.0004	0.00
0.5	1.0022	1.0019	0.03	1.0033	1.0034	0.02	1.0019	1.0020	0.01
1.0	1.0045	1.0040	0.05	1.0066	1.0066	0.01	1.0038	1.0039	0.01
1.5	1.0067	1.0061	0.06	1.0099	1.0095	0.04	1.0057	1.0058	0.01
2.0	1.0089	1.0081	0.08	1.0132	1.0127	0.05	1.0076	1.0076	0.00
2.5	1.0112	1.0103	0.09	1.0164	1.0161	0.03	1.0095	1.0093	0.02
3.0	1.0134	1.0124	0.10	1.0197	1.0194	0.03	1.0114	1.0113	0.00
3.5	1.0157	1.0145	0.11	1.0230	1.0227	0.03	1.0133	1.013	0.01
4.0	1.0179	1.0164	0.15	1.0263	1.0260	0.03	1.0152	1.0149	0.02
4.5	1.0201	1.0184	0.17	1.0296	1.0291	0.04	1.0171	1.0165	0.06
5.0	1.0224	1.0205	0.18	1.0329	1.0321	0.08	1.0189	1.0186	0.03
5.5	1.0246	1.0224	0.21	1.0362	1.0355	0.06	1.0208	1.0202	0.07
6.0	1.0268	1.0240	0.28	1.0395	1.0381	0.13	1.0227	1.0214	0.13
6.5	1.0291	1.0258	0.32	1.0428	1.0408	0.18	1.0246	1.0232	0.14
7.0	1.0313	1.0269	0.43	1.0460	1.0444	0.15	1.0265	1.0244	0.20

Table 8. Comparison of NBF values calculated using the fitting formula and MCNP6 code for 321 stainless steel at gamma-ray energies of 661.7 keV, 1173.2 keV, and 1332.5 keV

Thickness [cm]	Results for 661.7 keV			Results for 1173.2 keV			Results for 1332.5 keV		
	Fitting formula	MCNP6	RD [%]	Fitting formula	MCNP6	RD [%]	Fitting formula	MCNP6	RD [%]
0.1	1.0008	1.0008	0.01	1.0011	1.0012	0.00	1.0006	1.0007	0.00
0.5	1.0042	1.0040	0.02	1.0056	1.0056	0.00	1.0032	1.0033	0.01
1.0	1.0084	1.0082	0.02	1.0111	1.0110	0.01	1.0065	1.0068	0.03
1.5	1.0126	1.0123	0.03	1.0167	1.0167	0.01	1.0097	1.0101	0.04
2.0	1.0168	1.0167	0.01	1.0222	1.0223	0.01	1.0129	1.0135	0.06
2.5	1.0210	1.0207	0.03	1.0278	1.0281	0.03	1.0162	1.0168	0.06
3.0	1.0252	1.0251	0.01	1.0333	1.0337	0.03	1.0194	1.0203	0.09
3.5	1.0294	1.0292	0.02	1.0389	1.0395	0.06	1.0226	1.0235	0.08
4.0	1.0336	1.0330	0.05	1.0444	1.0450	0.06	1.0258	1.0266	0.07
4.5	1.0378	1.0363	0.14	1.0500	1.0504	0.04	1.0291	1.0291	0.00
5.0	1.0420	1.0408	0.11	1.0555	1.0554	0.01	1.0323	1.0318	0.05
5.5	1.0462	1.0454	0.08	1.0611	1.0615	0.04	1.0355	1.0349	0.07
6.0	1.0504	1.0497	0.07	1.0666	1.0670	0.04	1.0388	1.0378	0.09
6.5	1.0546	1.0540	0.06	1.0722	1.0726	0.04	1.0420	1.0404	0.15
7.0	1.0588	1.0577	0.11	1.0777	1.0784	0.07	1.0452	1.0445	0.07

Table 9. Comparison of NBF values calculated using the fitting formula and MCNP6 code for NRX 600 at gamma-ray energies of 661.7 keV, 1173.2 keV, and 1332.5 keV

Thickness [cm]	Results for 661.7 keV			Results for 1173.2 keV			Results for 1332.5 keV		
	Fitting formula	MCNP6	RD [%]	Fitting formula	MCNP6	RD [%]	Fitting formula	MCNP6	RD [%]
0.1	1.0009	1.0009	0.00	1.0012	1.0013	0.01	1.0007	1.0008	0.01
0.5	1.0047	1.0046	0.01	1.0060	1.0062	0.02	1.0035	1.0038	0.03
1.0	1.0094	1.0095	0.02	1.0120	1.0124	0.03	1.0070	1.0076	0.06
1.5	1.0140	1.0145	0.04	1.0180	1.0187	0.07	1.0105	1.0114	0.08
2.0	1.0187	1.0193	0.06	1.0240	1.0251	0.11	1.0140	1.0151	0.11
2.5	1.0234	1.0240	0.06	1.0300	1.0316	0.15	1.0175	1.0188	0.12
3.0	1.0281	1.0290	0.09	1.0360	1.0379	0.18	1.0210	1.0228	0.17
3.5	1.0328	1.0338	0.10	1.0420	1.0443	0.22	1.0245	1.0261	0.15
4.0	1.0374	1.0379	0.05	1.0480	1.0506	0.24	1.0281	1.0295	0.14
4.5	1.0421	1.0428	0.06	1.0541	1.0562	0.21	1.0316	1.0327	0.11
5.0	1.0468	1.0479	0.11	1.0601	1.0627	0.25	1.0351	1.0359	0.09
5.5	1.0515	1.0536	0.20	1.0661	1.0693	0.30	1.0386	1.0394	0.08
6.0	1.0562	1.0581	0.18	1.0721	1.0756	0.33	1.0421	1.0426	0.05
6.5	1.0608	1.0627	0.17	1.0781	1.0818	0.34	1.0456	1.0471	0.15
7.0	1.0655	1.0672	0.16	1.0841	1.0885	0.41	1.0491	1.0493	0.02

Table 10. Comparison of NBF values calculated using the fitting formula and MCNP6 code for C27000 copper alloy at gamma-ray energies of 661.7 keV, 1173.2 keV, and 1332.5 keV

Thickness [cm]	Results for 661.7 keV			Results for 1173.2 keV			Results for 1332.5 keV		
	Fitting formula	MCNP6	RD [%]	Fitting formula	MCNP6	RD [%]	Fitting formula	MCNP6	RD [%]
0.1	1.0010	1.0009	0.01	1.0012	1.0013	0.00	1.0007	1.0008	0.00
0.5	1.0049	1.0047	0.02	1.0061	1.0061	0.01	1.0036	1.0037	0.02
1.0	1.0099	1.0098	0.01	1.0121	1.0121	0.00	1.0071	1.0075	0.04
1.5	1.0148	1.0148	0.01	1.0182	1.0184	0.02	1.0107	1.0113	0.06
2.0	1.0197	1.0199	0.02	1.0242	1.0246	0.04	1.0142	1.0150	0.08
2.5	1.0246	1.0247	0.01	1.0303	1.0309	0.06	1.0178	1.0188	0.10
3.0	1.0296	1.0300	0.04	1.0363	1.0372	0.08	1.0213	1.0227	0.13
3.5	1.0345	1.0349	0.04	1.0424	1.0433	0.09	1.0249	1.0263	0.14
4.0	1.0394	1.0398	0.03	1.0484	1.0494	0.09	1.0284	1.0298	0.13
4.5	1.0443	1.0440	0.03	1.0545	1.0554	0.08	1.0320	1.0326	0.05
5.0	1.0493	1.0494	0.01	1.0606	1.0611	0.05	1.0356	1.0356	0.01
5.5	1.0542	1.0543	0.01	1.0666	1.0679	0.12	1.0391	1.0392	0.01
6.0	1.0591	1.0598	0.06	1.0727	1.0738	0.11	1.0427	1.0424	0.03
6.5	1.0640	1.0638	0.03	1.0787	1.0802	0.13	1.0462	1.0460	0.02
7.0	1.0690	1.0692	0.02	1.0848	1.0861	0.12	1.0498	1.0495	0.03

Table 11. Comparison of NBF values calculated using the fitting formula and MCNP6 code for bismuth germanate at gamma-ray energies of 661.7 keV, 1173.2 keV, and 1332.5 keV

Thickness [cm]	Results for 661.7 keV			Results for 1173.2 keV			Results for 1332.5 keV		
	Fitting formula	MCNP6	RD [%]	Fitting formula	MCNP6	RD [%]	Fitting formula	MCNP6	RD [%]
0.1	1.0024	1.0020	0.03	1.0018	1.0017	0.00	1.0011	1.0010	0.01
0.5	1.0119	1.0103	0.16	1.0089	1.0083	0.06	1.0053	1.0051	0.03
1.0	1.0238	1.0209	0.28	1.0177	1.0162	0.14	1.0106	1.0102	0.04
1.5	1.0357	1.0318	0.38	1.0266	1.0247	0.18	1.0159	1.0151	0.08
2.0	1.0475	1.0426	0.48	1.0354	1.0334	0.20	1.0212	1.0204	0.08
2.5	1.0594	1.0538	0.53	1.0443	1.0421	0.21	1.0265	1.0256	0.09
3.0	1.0713	1.0644	0.65	1.0531	1.0504	0.26	1.0319	1.0307	0.11
3.5	1.0832	1.0748	0.78	1.0620	1.0596	0.23	1.0372	1.0361	0.10
4.0	1.0951	1.0861	0.83	1.0709	1.0676	0.30	1.0425	1.0407	0.17
4.5	1.1070	1.0982	0.80	1.0797	1.0766	0.29	1.0478	1.0456	0.21
5.0	1.1188	1.1099	0.81	1.0886	1.0847	0.36	1.0531	1.0503	0.27
5.5	1.1307	1.1206	0.90	1.0974	1.0931	0.40	1.0584	1.0544	0.38
6.0	1.1426	1.1318	0.95	1.1063	1.1028	0.32	1.0637	1.0590	0.45
6.5	1.1545	1.1437	0.94	1.1151	1.1113	0.35	1.0690	1.0637	0.50
7.0	1.1664	1.1557	0.92	1.1240	1.1207	0.30	1.0743	1.0684	0.55

Table 12. Comparison of NBF values calculated using the fitting formula and MCNP6 code for lead tungstate at gamma-ray energies of 661.7 keV, 1173.2 keV, and 1332.5 keV

Thickness [cm]	Results for 661.7 keV			Results for 1173.2 keV			Results for 1332.5 keV		
	Fitting formula	MCNP6	RD [%]	Fitting formula	MCNP6	RD [%]	Fitting formula	MCNP6	RD [%]
0.1	1.0028	1.0025	0.03	1.0021	1.0020	0.01	1.0013	1.0012	0.00
0.5	1.0142	1.0129	0.12	1.0105	1.0100	0.05	1.0063	1.0061	0.01
1.0	1.0283	1.0260	0.23	1.0210	1.0195	0.15	1.0125	1.0123	0.02
1.5	1.0425	1.0397	0.26	1.0315	1.0300	0.14	1.0188	1.0185	0.03
2.0	1.0566	1.0533	0.32	1.0420	1.0404	0.15	1.0251	1.0249	0.02
2.5	1.0708	1.0669	0.36	1.0525	1.0509	0.16	1.0313	1.0313	0.01
3.0	1.0849	1.0803	0.43	1.0630	1.0618	0.12	1.0376	1.0378	0.02
3.5	1.0991	1.0943	0.44	1.0735	1.0716	0.18	1.0439	1.0437	0.01
4.0	1.1132	1.1095	0.34	1.0840	1.0826	0.13	1.0501	1.0496	0.05
4.5	1.1274	1.1235	0.34	1.0945	1.0921	0.22	1.0564	1.0552	0.12
5.0	1.1415	1.1386	0.26	1.1050	1.1033	0.15	1.0627	1.0606	0.20
5.5	1.1557	1.1532	0.22	1.1155	1.1135	0.18	1.0689	1.0662	0.26
6.0	1.1699	1.1691	0.07	1.1260	1.1252	0.08	1.0752	1.0723	0.28
6.5	1.1840	1.1846	0.05	1.1365	1.1359	0.06	1.0815	1.0792	0.21
7.0	1.1982	1.1996	0.12	1.1470	1.1474	0.03	1.0877	1.0839	0.35

CONCLUSIONS

In the present study, we successfully developed a novel method that combines Monte Carlo simulations with fitting formula to calculate the NBF in GT measurements using narrow beam geometry. The advantage of using Monte Carlo simulations with the MCNP6 code lies in its convenience, flexibility and precision for computing the NBF across various geometrical configurations, material types, and gamma-ray energies. The fitting formula, derived from simulation data, enables the rapid calculation of the NBF for any sample, given that the sample thickness, mass density, and atomic number are precisely known. The RD between the NBF values calculated using the fitting formula and those obtained with the MCNP6 code were consistently found to be less than 1 % across all the investigated cases. These results are sufficient to confirm the high accuracy of the proposed fitting formula in calculating the NBF.

Besides, this study provides practical insights into NBF values in GT measurements using narrow beam geometry, across various material types, sample thicknesses, and gamma-ray energies. It is important to emphasize that the influence of the NBF cannot be ignored, even in well-collimated GT geometries. Indeed, the NBF values obtained from the MCNP6 simulations can exceed 1.03 for samples with substantial thicknesses, high atomic number and large mass density. Even, the maximum NBF value can reach up to 1.34 for lead material at an energy of 661.7 keV and a sample thickness of 7 cm. Note that an NBF value of 1.03 indicates that the total intensity of gamma rays incident on the detector (I) is 3 % greater than the intensity of the transmitted gamma rays (I_{Tran}). This can lead to significant errors in measurement results for applications based on GT measurements using narrow beam geometries if the NBF is not taken into account. Therefore, our method should be useful for applications requiring high precision, such as measuring thickness, mass density, and MAC.

ACKNOWLEDGMENT

This research is funded by Vietnam National University, Ho Chi Minh City (VNU-HCM) under grant number C2022-18-07.

AUTHORS' CONTRIBUTIONS

H. D. Chuong: proposing the research idea, developing theoretical background, building simulation configuration, writing original manuscript, and project administration. L. T. N. Trang: literature reviewing, running simulations, data analysis, correcting manuscript. N. T. T. Linh: data analysis, correcting manuscript. V. H. Nguyen: running simulations, correcting manuscript. T. T. Thanh: providing MCNP6 code, correcting manuscript.

ORCID NO

H. D. Chuong: 0000-0003-3903-6388
L. T. N. Trang: 0000-0002-9354-022X
N. T. T. Linh: 0000-0002-7706-8391
V. H. Nguyen: 0009-0007-2828-6142
T. T. Thanh: 0000-0002-9866-4926

REFERENCES

[1] Shirakawa, Y., A Build-Up Treatment for Thickness Gauging of Steel Plates Based on Gamma-Ray Trans-

mission, *Appl Radiat Isot, 53* (2000), Nov., pp. 581-586
[2] Chuong, H. D., *et al*., Thickness Determination of Material Plates by Gamma-Ray Transmission Technique Using Calibration Curves Constructed from Monte Carlo Simulation, *Radiat Phys Chem, 190* (2022), 109821
[3] Trang, L. T. N., *et al*., An Approach Based on Gamma-Ray Transmission Technique and Artificial Neural Network for Accurately Measuring the Thickness of Various Materials, *Nucl Technol Radiat, 39* (2024), 2, pp. 98-110
[4] Chuong, H. D., *et al*., A Novel Approach for Constructing the Calibration Curve Applied in Determining the Thickness of Different Types of Materials, *Radiat Phys Chem, 214* (2024), 111282
[5] Khorsandi, M., *et al*., Developing a Gamma Ray Fluid Densitometer in Petroleum Products Monitoring Applications Using Artificial Neural Network, *Radiat Measure, 59* (2013), Dec., pp. 183-187
[6] Beigzadeh, A. M., *et al*., Design and Improvement of a Simple and Easy-To-Use Gamma-Ray Densitometer for Application in Wood Industry, *Measure, 138* (2019), May, pp. 157-161
[7] Chuong, H. D., *et al*., Monte Carlo Simulation Combined with Experimental Measurements Based on Gamma Transmission Technique for Determining the Density of Liquid, *Radiat Phys Chem, 179* (2021), 109216
[8] Linh, N. T. T., *et al*., Combining Monte Carlo Simulation and Experimental Data for Determining the Density of Polymer Materials in Gamma Scattering and Gamma Transmission Measurements, *J Radioanal Nucl Chem, 332* (2023), May, pp. 2929-2943
[9] Oliveira, J. M., *et al*., Porosity Measurement of Solid Pharmaceutical Dosage forms by Gamma-Ray Transmission, *Appl Radiat Isot, 68* (2010), Dec., pp. 2223-2228
[10] Siengsanoh, K., *et al*., Porosity Investigation of Bricks by Gamma-Ray Transmission Measurement, *Mater Today Proc, 43* (2021), 3, pp. 2612-2617
[11] Demir, D., *et al*., Determination of Photon Attenuation Coefficient, Porosity and Field Capacity of Soil by Gamma-Ray Transmission for 60, 356 and 662 keV Gamma Rays, *Appl Radiat Isot, 66* (2008), Dec., pp. 1834-1837
[12] Medhat, M. E., Application of Gamma-Ray Transmission Method for Study the Properties of Cultivated Soil, *Ann Nucl Energy, 40* (2012), Feb., pp. 53-59
[13] Singla, A., *et al*., Investigation of Impact of Soil Texture, Depth and Gamma Ray Energy on the Mass Attenuation Coefficient and Determination of Soil Bulk Density Using Gamma-Ray Spectrometry, *Radiat Phys Chem, 216* (2024), 111400
[14] Vejdani-Noghreiyan, A., *et al*., Theoretical and Experimental Determination of Mass Attenuation Coefficients of Lead-Based Ceramics and Their Comparison with Simulation, *Nucl Technol Radiat, 31* (2016), 2, pp. 142-149
[15] Shams, T., *et al.*, Investigation of Gamma Radiation Attenuation in Heavy Concrete Shields Containing Hematite and Barite Aggregates in Multi-Layered and Mixed Forms, *Constr Build Mater, 182* (2018), Sept., pp. 35-42
[16] Nagaraja, N., *et al*., Radiation Shielding Properties of Silicon Polymers, *Radiat Phys Chem, 171* (2020), 108723
[17] Taqi, A. H., *et al*., Shielding Properties of Cu-Sn-Pb Alloy by Geant4, XCOM and Experimental Data, *Mater Today Commun, 26* (2021), 101996
[18] Elsheikh, N. A. A., Monte Carlo Gamma Transmission Model for Characterization of Multi-Gamma Shielding Parameters of Some Heavy Metal Oxide Glasses, *Nucl Technol Radiat, 36* (2021), 4, pp. 338-345
[19] Alhamdi, W. A., *et al*., Investigation of the Gamma Shielding Efficiency Reduction by Depositing PbO and MnO_2 Composition on Various Types of Substrates, *Nucl Technol Radiat, 38* (2023), 3, pp. 179-186
[20] Saleh, A., *et al*., An Appropriate Balance of Mechanical and Ionized Radiation Shielding Performance Across Some Tin Binary Alloys: A Comparative Investigation, *Radiat Phys Chem, 221* (2024), 111726
[21] Almuqrin, A. H., *et al*., An Experimental and Theoretical Study to Evaluate Al_2O_3-PbO-B_2O_3-SiO_2-BaO Radiation Shielding Properties, *Radiat Phys Chem, 222* (2024), 111824
[22] Gayer, A., *et al*., Study of the Effect of Scattered Photons on Attenuation Coefficient Measurements, *Nucl Instrum Methods Phys Res, 220* (1984), Mar., pp. 525-530
[23] Mann, K. S., Measurement of Exposure Buildup Factors: the Influence of Scattered Photons on Gamma-Ray Attenuation Coefficients, *Nucl Instrum Methods Phys Res A, 877* (2018), Jan., pp. 1-8
[24] White, G. R., The Penetration and Diffusion of Co^{60} Gamma-Rays in Water Using Spherical Geometry, *Phys Rev, 80* (1950), Oct., pp. 154-156
[25] Das, A., *et al*., Development of a New Monte Carlo Based Transport Code to Calculate Photon Exposure Build-Up Factors in Various Shielding Arrangements, *Radiat Phys Chem, 194* (2022), 110028
[26] Sardari, D., *et al*., Evaluation of Gamma Ray Buildup Factor Data in Water with MCNP4C Code, *Ann Nucl Energy, 38* (2011), Feb.-Mar., pp. 628-631
[27] Rafiei, M. M., *et al*., A Detailed Investigation of Gamma-Ray Energy Absorption and Dose Buildup Factor for Soft Tissue and Tissue Equivalents Using Monte Carlo Simulation, *Radiat Phys Chem, 177* (2020), 109118
[28] Alda'ajeh, M. M., *et al*., Determination of Buildup Factors for Some Human Tissues Using Both MCNP5 and Phy-X/PSD, *Nucl Eng Technol, 55* (2023), Dec., pp. 4426-4430
[29] Goorley, T., *et al*., Features of MCNP6, *Ann Nucl Energy, 87* (2016), Jan., pp. 772-783
[30] Taylor, J. J., Application of Gamma Ray Build-Up Data to Shield Design, United States, WAPD-RM-217, 1954
[31] Chilton, A.B., Tchebycheff-fitted Berger Coefficients for Eisenhauer-Simmons Gamma-Ray Buildup Factors in Ordinary Concrete, *Nucl Sci Eng, 69* (1979), 3, pp. 436-438
[32] Harima, Y., *et al*., An Approximation of γ-Ray Buildup Factors by Geometrical Progression, *Nucl Eng Des, 23* (1972), Nov., pp. 209-227
[33] Podgorsak, E. B., *Radiation Physics for Medical Physicists*, Springer Berlin, Heidelberg, Germany, 2010
[34] ***, IUPAC Commission on Isotopic Abundances and Atomic Weights, https://iupac.qmul.ac.uk/AtWt/ (accessed on 15 May 2024)
[35] Duvauchelle, P., *et al*., Effective Atomic Number in the Rayleigh to Compton Scattering Ratio, *Nucl Instrum Methods Phys Res B, 155* (1999), Aug., pp. 221-228
[36] Singh, M. P., *et al.*, Measurement of Effective Atomic number of Composite Materials Using Scattering of γ-Rays, *Nucl Instrum Methods Phys Res A, 580* (2007), Sept., pp. 50-53
[37] Manohara, S. R., *et al*., On the Effective Atomic Number and Electron Density: A Comprehensive Set of Formulas for All Types of Materials and Energies

Above 1 keV, *Nucl Instrum Methods Phys Res B, 266* (2008), Sept., pp. 3906-3912
[38] Thanh, T. T., *et al*., Study of Different Methods to Estimate the Rayleigh to Compton Scattering Ratio and the Effective Atomic Number ($10 < Z < 30$) Using Si(Li) Detector, *Nucl Instrum Methods Phys Res A, 969* (2020), July, 163995
[39] Chuong, H. D., *et al*., Validation of Gamma Scanning Method for Optimizing NaI(Tl) Detector Model in Monte Carlo Simulation, *Appl Radiat Isot, 149* (2019), July, pp. 1-8
[40] Berger, M. J., *et al*., NIST XCOM: Photon Cross Sections Database, https://www.nist.gov/pml/xcom-photon-cross-sections-database (accessed on 15 May 2024)

Received on July 19, 2024
Accepted on December 20, 2024

Хујњ Дињ ЧУЕНГ, Ле Ти Нгок ТРАНГ, Нгујен Ти Трук ЛИЊ,
Во Хоанг НГУЈЕН, Тран Тиен ТАЊ

НОВА МЕТОДА ЗА ИЗРАЧУНАВАЊЕ ФАКТОРА УГРАДЊЕ У МЕРЕЊИМА ПРЕНОСА ГАМА ЗРАЧЕЊА КОРИШЋЕЊЕМ ГЕОМЕТРИЈЕ УСКОГ СНОПА

Представљена је нова метода за израчунавање фактора уградње за произвољне материјале у мерењима преноса гама зрачења коришћењем уске геометрије зрачења. Коришћен је MCNP6 код за симулацију транспорта фотона унутар колимиране конфигурације преноса, која је укључивала NaI(Tl) сцинтилациони детектор упарен са ^{137}Cs или ^{60}Co радиоактивним извором. Из ових симулација, израчунате су вредности фактора уградње за различите материјале при енергијама гама зрака од 661.7 keV, 1173.2 keV и 1332.5 keV, са дебљинама узорка у распону од 0.1 cm до 7.0 cm. Код сваке специфицне енергије гама зрачења и материјала, вредности фактора уградње показале су јаку линеарну везу са дебљином узорка. Нагиб ових линеарних зависности може се изразити као производ густине масе и кубне полиномијалне функције атомског броја. На основу ових налаза, изведена је одговарајућа формула за израчунавање фактора уградње коришћењем улазних променљивих: дебљине узорка, густине масе и атомског броја. Тачност апроксимативне формуле процењена је упоређивањем њених резултата са вредностима фактора уградње израчунатим MCNP6 кодом. Поређење је показало релативна одступања испод 1 % за све истражене случајеве, што показује високу тачност и поузданост апроксимативне формуле.

Кључне речи: пренос гама зрачења, Монте Карло симулација, MCNP6, NaI(Tl) детектор, геометрија уског снопа, фактор уградње